



**HAL**  
open science

## **GaN class E Wireless Power Transfer system: a new design method relying on the advanced modeling of parasitic elements**

Nathis Cote, Nicolas Garraud, Léo Sterna, Pierre Perichon, François Frassati, Sebastien Boisseau

### ► To cite this version:

Nathis Cote, Nicolas Garraud, Léo Sterna, Pierre Perichon, François Frassati, et al.. GaN class E Wireless Power Transfer system: a new design method relying on the advanced modeling of parasitic elements. powerMEMS - 2023 IEEE 22nd International Conference on Micro and Nanotechnology for Power Generation and Energy Conversion Applications, Dec 2023, Abu Dhabi, Saudi Arabia. pp.30-32, 10.1109/PowerMEMS59329.2023.10417504 . cea-04592850

**HAL Id: cea-04592850**

**<https://cea.hal.science/cea-04592850>**

Submitted on 29 May 2024

**HAL** is a multi-disciplinary open access archive for the deposit and dissemination of scientific research documents, whether they are published or not. The documents may come from teaching and research institutions in France or abroad, or from public or private research centers.

L'archive ouverte pluridisciplinaire **HAL**, est destinée au dépôt et à la diffusion de documents scientifiques de niveau recherche, publiés ou non, émanant des établissements d'enseignement et de recherche français ou étrangers, des laboratoires publics ou privés.

# GAN CLASS E WIRELESS POWER TRANSFER SYSTEM: A NEW DESIGN METHOD RELYING ON THE ADVANCED MODELING OF PARASITIC ELEMENTS

*Nathis Côte, Nicolas Garraud, Léo Sterna, Pierre Périchon, François Frassati  
and Sébastien Boisseau*

CEA-Leti, Université Grenoble Alpes, F-38000 Grenoble, France

## ABSTRACT

We report the design, the simulation and the characterization of a 13.56 MHz resonant inductive coupling wireless power transfer (WPT) system based on a class E inverter. The main benefit of a class E WPT system is the small amount of components needed while achieving good efficiency. An analytical model of the system is proposed and a new design method is reported. The fabricated system shows an efficiency of 76 % for a transmitted power of 3.4 W.

## KEYWORDS

Wireless Power Transfer, inductive coupling, class E, inverter, GaN, Non-Mating Connectors (NMC)

## INTRODUCTION

Wireless power transfer (WPT) is widely used to remotely power autonomous systems in applications where no contact is required or desired (phone, drone, car...) [1]. WPT is also used for non-mating connectors to avoid electrical contact corrosion or wear in harsh industrial settings for example [2]. Resonant inductive coupling is one method widely used to efficiently transfer energy from a transmitter coil to a receiver coil [3]. An inductive resonant WPT system (Figure 1) is composed of a DC power supply, an inverter, a coupler, a rectifier and a load [4].

The system is highly dependent of the inverter as it provides the high frequency signal matched with the resonant coupler. However, at multi-MHz frequencies, inverters are complex to design because of the parasitic components. Several inverter technologies are used. The most common in the MHz range are class E [5] and class  $\phi_2$  [6] inverters. Switching losses are reduced by using a transistor under Zero-Voltage Switching (ZVS) conditions. The class  $\phi_2$  inverter, derived from the class E, has the particularity to lower the voltage constraint on the transistor by using a resonant branch tuned at the second harmonic of the operating frequency. However, this topology is more complex and use more components.

In this paper, the design, the advanced simulation and the characterization of a compact WPT system based on a

13.56 MHz class E inverter are presented. The transmitter coil inductance in a class E WPT system corresponds in part to the inductors  $L_1$  and  $L_2$  of a class E inverter (Figure 2). The coil is therefore mutualized, reducing the amount of components and the size of the system.

## PRE-DESIGN OF THE CLASS E WPT SYSTEM

### Basics on class E inverters

A class E inverter (Figure 2) is composed of:

- A choke inductor  $L_{choke}$  to get DC current
- A switch  $S_1$  to generate the AC signal at  $f_0$
- A capacitor  $C_1$  and an inductor  $L_1$  to set the zero-voltage switching (ZVS)
- A capacitor  $C_2$  and an inductor  $L_2$  to create a resonance at the given frequency  $f_0$
- A load resistor  $R$

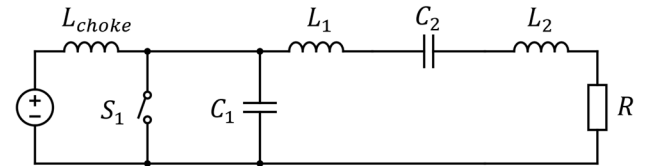


Figure 2: Schematic of a class E inverter.

The switch  $S_1$  is driven at  $f_0$  with a duty cycle  $D$ . The components  $C_1$  and  $L_1$  are set to achieve ZVS with equations from [7]. The shape of the output signal depends highly on the quality factor  $Q = \frac{\omega_0 L_2}{R}$  of the inverter output resonant branch. The higher the quality factor, the smallest the harmonics and thus the better the sinewave is. A decent sinus is obtained for quality factors higher than 10 [7].

### Similarities between class E inverters and class E WPT systems

A class E WPT system can either include an impedance matching network or integrate the transmitter coil as part of the inductors  $L_1$  and  $L_2$  of the class E inverter (Figure 2). The latter is used in this work to mutualize the coil, reduce the amount of component and the size of the system.

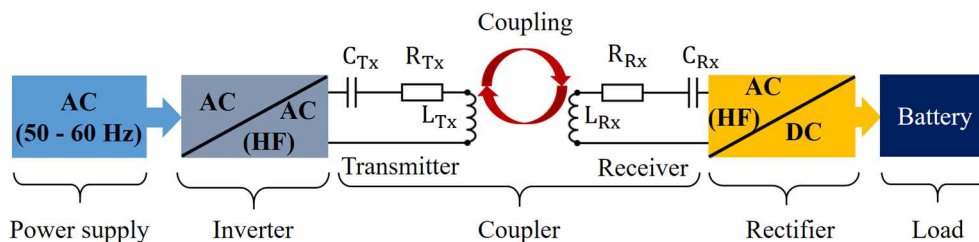


Figure 1: Five parts composing a WPT system.

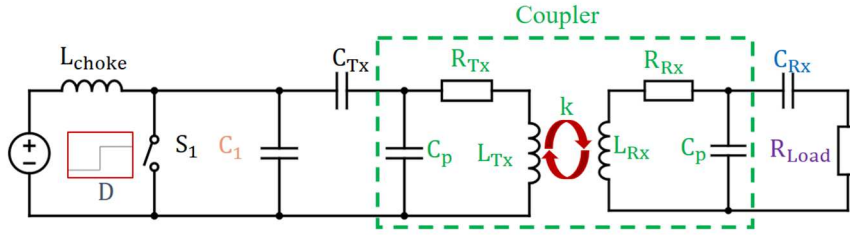


Figure 2: Schematic of a class E WPT system, including some parasitic elements.

Similarities can be found between the class E inverter and the class E WPT circuit, and equivalences be established. The load  $R$  in the equivalent class E inverter (Figure 2) is composed of the real part of the reflected impedance from the secondary side of the coupler ( $R_x$ ) and the losses of the transmitting coil ( $T_x$ ):

$$R = R_{Tx} + R_{reflected} \quad (1)$$

Likewise,  $L_1$  and  $L_2$  depend on the Tx coil impedance and the imaginary part of the reflected impedance:

$$L_1 + L_2 = L_{Tx} + \frac{X_{reflected}}{\omega} \quad (2)$$

### Pre-design of a class E WPT system

In a first time, the coupler is designed independently based on constraints from the application (topology, size...) and in order to achieve a high coupling with low losses and parasitic capacitances. The coupler used in this work (Figure 3) is composed of a 16.0-mm-long 21.0-mm-wide transmitter coil ( $L_{Tx} = 385$  nH,  $R_{Tx} = 0.27 \Omega$ ) and a concentric 13.4-mm-long 15.0-mm-wide receiver coil ( $L_{Rx} = 255$  nH,  $R_{Rx} = 0.18 \Omega$ ) with a coupling  $k$  of 59 % and low parasitic capacitances  $C_p = 5$  pF.

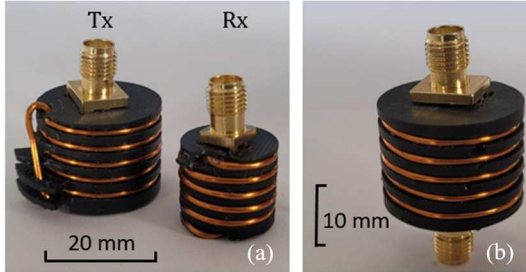


Figure 3: Tx and Rx coils (a), and assembled coupler (b).

The coupler efficiency can be estimated by

$\eta_{coupler} = \frac{R_{lossless}}{R}$ , with  $R_{lossless}$  the load resistance on the equivalent class E inverter with the assumption of a lossless coupler.

In a second time, the class E inverter, considered perfect with no parasitic elements in the analytical model, is designed based on the coupler parameters and previous equations and conditions. To simplify this work, a working load of  $R_{Load} = 50 \Omega$  and a duty cycle of  $D = 0.5$  are selected. In this case, equations (1) and (2) only depend on  $C_{Rx}$ . Because the coupler is highly coupled, it is important to monitor the impedance at the second harmonic as frequency splitting may appear [6]. Also, the switch is a GaN transistor (GS61004B from GaN Systems) presenting a high parasitic capacitance  $C_{oss}$  varying with the voltage (300 pF around 0 V, 150 pF around 20 V). Therefore,  $C_1$

has to be chosen high enough to lower the effects of  $C_{oss}$  variations ( $C_{oss} \ll C_1$ ), as observed in Figure 4.

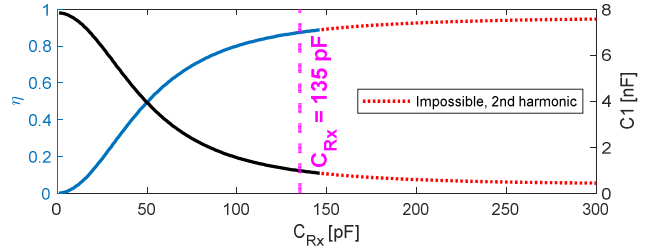


Figure 4: Coupler efficiency and  $C_1$  as a function of  $C_{Rx}$ .

An acceptable compromise is found for  $C_{Rx} = 135$  pF with a coupler theoretical efficiency  $\eta_{coupler}$  of 87.3 %. Such parameters lead to  $C_1 = 979$  pF,  $R = 2.20 \Omega$  and  $L_1 + L_2 = 421$  nH (at 13.56 MHz).

## FINE TUNING WITH NUMERICAL SIMULATIONS

### Electromagnetic simulations

Simple Spice simulations using the spice model of the GaN transistor and the 2-port S-parameter model of the coupler are not accurate enough because of the high operating frequency and parasitic elements in the PCB. Therefore, electromagnetic simulations are first performed on PePro (ADS Keysight) to model the circuit presented in Figure 5.

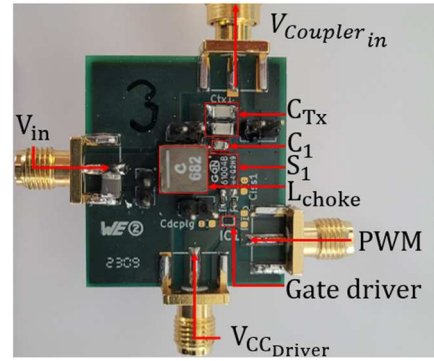


Figure 5: PCB of the class E inverter for WPT.

### Spice simulations

Both S-matrices, extracted from PePro simulations, and components characteristics, obtained from datasheet or measurements with a high frequency impedance analyzer, are used to build a Spice model on ADS Keysight. Performances are improved by slightly tuning the components values (for example  $C_1$ , with the precise model of the GaN and its parasitic capacitance). The overall simulated efficiency of the system  $\eta_{system}$  is 79.3 %, with losses occurring mainly in the coupler (50 %) and the switch (20 %) (Figure 6).

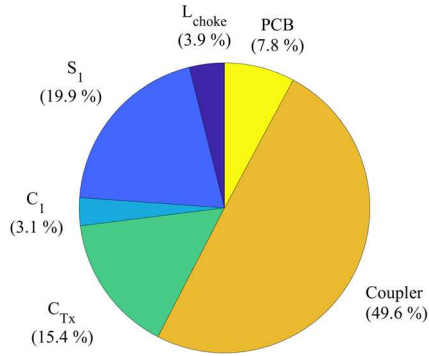


Figure 6: Losses repartition

The losses in the switch are mainly due to the on-resistance of  $S_1$ , which increases with the heat in the component. It is therefore necessary to pay particular attention to the thermal dissipation of this component.

## RESULTS AND DISCUSSIONS

The class E WPT circuit (Figure 7) is assembled using the coupler, the class E inverter and a second PCB with  $C_{Rx}$  and  $R_{Load}$ . The system is characterized at low voltages ( $V_{in} \leq 5$  V) to prevent overheating and failure of the GaN transistor as heat dissipation elements were not taken into account during modeling.

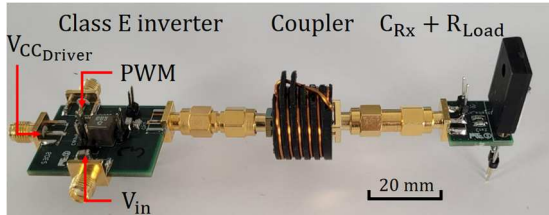


Figure 7: Class E WPT system.

Voltages are measured using isolated probes. This actual system presents a total efficiency of 76.0 % for an output power of 3.4 W. The ZVS is acceptable with small ripples during the on-state as shown in Figure 8.

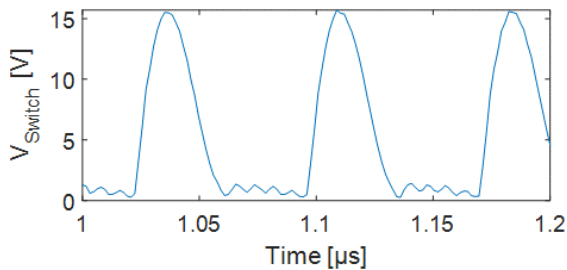


Figure 8: Voltage across the switch during switching.

Table 1: Performances comparison for  $V_{in} = 5$  V.

	$P_{in} = \text{mean}(V_{in}I_{in})$	$\frac{P_{out} = V_{out}^2(RMS)}{R_{Load}}$	$\eta_{sys} = \frac{P_{out}}{P_{in}}$
Theory	6.55 W	5.73 W	87.3 %
Simulations	4.52 W	3.58 W	79.3 %
Prototype	4.50 W	3.42 W	76.0 %

As shown in Table 1, measurements are in good agreement with simulations (mismatch of 4 % between advanced simulations and experimental results). The gap with the

analytical model is greater (15%) since it does not take into account losses of the converter and its components. Therefore, the analytical model is primarily used to globally dimension the circuit, while simulations are used to refine the model and the operating point.

## CONCLUSION AND PROSPECTS

We present in this paper the design of a 13.56 MHz class E WPT system transmitting 3.4 W at 76 % efficiency. A new design guide for multi-MHz WPT systems is proposed based on an analytical model. Precise electromagnetic simulations are performed to finely optimize the components. Measurements performed on a fabricated prototype show a good agreement with simulations.

The next steps are to characterize the system at higher voltages, optimize the coupler in order to increase the efficiency and include the losses of the class E inverter in the analytical model.

This new design method paves the way towards high efficiency WPT systems thanks to an advanced understanding of losses and parasitic behaviors. In the future, a prototype operating at higher power will be designed.

## REFERENCES

- [1] S. D. Barman, A. W. Reza, N. Kumar, Md. E. Karim, and A. B. Munir, "Wireless powering by magnetic resonant coupling: Recent trends in wireless power transfer system and its applications," *Renew. Sustain. Energy Rev.*, vol. 51, pp. 1525–1552, Nov. 2015, doi: 10.1016/j.rser.2015.07.031.
- [2] J. Benjestorf, "A New Trend In Connectivity: Sharing content over multiple channels.," p. 7.
- [3] O. Okoyeigbo, A. A. Olajube, O. Shobayo, A. Aligbe, and A. E. Ibhaze, "Wireless power transfer: a review," *IOP Conf. Ser. Earth Environ. Sci.*, vol. 655, no. 1, p. 012032, Feb. 2021, doi: 10.1088/1755-1315/655/1/012032.
- [4] S. Chatterjee, A. Iyer, C. Bharatiraja, I. Vaghasia, and V. Rajesh, "Design Optimisation for an Efficient Wireless Power Transfer System for Electric Vehicles," *Energy Procedia*, vol. 117, pp. 1015–1023, Jun. 2017, doi: 10.1016/j.egypro.2017.05.223.
- [5] M. Kazimierczuk and K. Puczek, "Exact analysis of class E tuned power amplifier at any Q and switch duty cycle," *IEEE Trans. Circuits Syst.*, vol. 34, no. 2, pp. 149–159, Feb. 1987, doi: 10.1109/TCS.1987.1086114.
- [6] K. Kitazawa, X. Wei, A. Katsuki, and M. Hirokawa, "Analysis and Design of the Class- $\Phi_2$  Inverter," in *IECON 2018 - 44th Annual Conference of the IEEE Industrial Electronics Society*, Oct. 2018, pp. 1023–1028. doi: 10.1109/IECON.2018.8592487.
- [7] M. Kazimierczuk, "Resonant Power Converters, 2nd Edition | Wiley." Accessed: Apr. 25, 2023. [Online]. Available: <https://www.wiley.com/en-kr/Resonant+Power+Converters,+2nd+Edition-p-9780470905388>

## CONTACT

\*N. Côte, tel: +33 4 38 78 01 57; [nathis.cote@cea.fr](mailto:nathis.cote@cea.fr)